ANL-7689

Argonne National Laboratory

ON THE MULTIPLE SCATTERING OF GAMMA RADIATION

by

P. J. Brockwell and H. Greenspan

Printed in the United States of America
Available from
National Technical Information Service
U.S. Department of Commerce
Springfield, Virginia 22151
Price: Printed Copy $3.00; Microfiche $0.65

ANL-7689
Mathematics and Computers

ARGONNE NATIONAL LABORATORY
9700 South Cass Avenue
Argonne, Illinois 60439

ON THE MULTIPLE SCATTERING OF GAMMA RADIATION

by

P. J. Brockwell and H. Greenspan*

Applied Mathematics Division

June 1970

---

*Now with Applied Physics Division.

TABLE OF CONTENTS

LIST OF FIGURES

LIST OF FIGURES

ON THE MULTIPLE SCATTERING OF GAMMA RADIATION

by

P. J. Brockwell and H. Greenspan

ABSTRACT

A method has been devised to calculate the joint and marginal distribution of the emergent wavelength λ and angle of emergence θ, given a quantum of gamma radiation incident on the left face of the slab $\{\underset{\sim}{x}: 0 \le x \le a\}$ with wavelength λ_0 and angle of incidence θ_0. The method has been applied in this instance to scattering cross sections $\sigma_\lambda(\theta)$ as given by the Klein-Nishina formula, but can be used with any other specified scattering law. Results obtained compare well with Monte Carlo calculations for marginal distributions, but the developed procedure yields more information regarding joint distributions for the same effort.

I. INTRODUCTION

Consider a quantum of gamma radiation with wavelength λ moving through a homogeneous slab of scattering material. Independently of the previous history of the particle, the probability that it makes a collision in the small length of path ds is given by $\Sigma_\lambda\, ds + o(ds)$, and the probability, conditional upon a collision, that it is deflected through angle θ into the element of solid angle $d\Omega$, is given by $\Sigma_\lambda^{-1}\, \sigma_\lambda(\theta)\, d\Omega + o(d\Omega)$. Here, $\sigma_\lambda(\theta)$ is given by the Klein-Nishina formula,

$$\sigma_\lambda(\theta) = \frac{3}{16\pi} \frac{\lambda^2}{\lambda'^2} \left(\frac{\lambda}{\lambda'} + \frac{\lambda'}{\lambda} - \sin^2 \theta \right), \tag{1.1}$$

where λ', the wavelength after deflection through the angle θ, is related to λ and θ by the Compton relation,

$$\lambda' = \lambda + 1 - \cos \theta. \tag{1.2}$$

The scattering cross section (or inverse mean free path) is expressed in terms of $\sigma_\lambda(\theta)$ by

$$\Sigma_\lambda = 2\pi \int_{-1}^{1} \sigma_\lambda(\theta) d(\cos \theta). \tag{1.3}$$

The probability of more than one collision in distance ds is assumed to be $o(ds)$. Notice that as λ tends to ∞, Eq. 1.1 becomes

$$\sigma_\infty(\theta) = \frac{3}{16\pi}(1 + \cos^2\theta), \tag{1.4}$$

which is just the Rayleigh scattering law for low-energy quanta. In writing Eqs. 1.1-1.4, we are assuming that wavelengths are measured in Compton units (1 C.u. $\simeq 2.426 \times 10^{-10}$ cm) and that all other distances are measured in units of the limiting mean free path as λ tends to ∞, namely Σ_∞^{-1}. (If N is the number of scattering electrons per unit volume of the medium and σ_e is the known cross section per electron for scattering of low-energy quanta, viz., one Thomson unit or 0.665 barn, then, $\Sigma_\infty = N\sigma_e$.) In terms of these units, Eqs. 1.2-1.4 describe the scattering of gamma-ray quanta by free (or loosely bound) electrons in the absence of photoelectric absorption or pair production. It would not be difficult to modify our calculations to take these effects into account. However, we shall neglect them in the present report and consider only the effects of multiple scattering.

The problem with which we shall be specifically concerned is the following: Given a quantum of radiation incident on the left face of the slab $\{\underset{\sim}{x}: 0 \leq x \leq a\}$ with wavelength λ_0 and angle of incidence θ_0, what is the joint distribution of the emergent wavelength λ and angle of emergence θ? (The angles of incidence and emergence are measured from the x-axis, which is normal to the slab faces.)

Even if attention were restricted to the low-energy approximation (Eq. 1.4), rather than the Klein-Nishina formula (Eq. 1.2), a completely analytical treatment of multiple scattering would be extremely difficult indeed. Chandrasekhar[4] devised an approximate method for determining the distribution of emergent wavelength when the differential cross section is isotropic, viz., $\sigma_\lambda(\theta) = 1/(4\pi)$, and this method was later used by O'Rourke[7] for similar problems. The case $\sigma_\lambda(\theta) = [3/(16\pi)][1 + \cos^2\theta]$ was studied by Brockwell,[1,2] using a discretization of the set of possible directions of motion. In this approximation, the photons are restricted to move in one of a set of 30 directions determined by the lines joining the center of a regular icosahedron to the midpoints of its edges. Studies of the more realistic case in which $\sigma_\lambda(\theta)$ is given by the Klein-Nishina formula (Eq. 1.2) are usually made by means of Monte Carlo techniques (see Fano, Spencer, and Berger[5]).

The purpose of this report is to extend the method of Brockwell to deal with Klein-Nishina scattering. We shall see in Sect. VI that our method agrees well with the results of Monte Carlo calculations. For a given amount of computation, however, we obtain a great deal more information regarding the joint distribution of emergent energy and direction of scattered photons than is obtained from the Monte Carlo calculations. The method we shall describe extends in an obvious way to problems with other energy-dependent scattering laws.

II. THE BACKWARD KOLMOGOROV EQUATION AND ITS DISCRETE APPROXIMATION

In slab geometry, it is convenient to characterize the state of a photon by its x-coordinate (measured normally into the slab from its left face), its wavelength λ (measured in Compton units), and the angle made by its direction

of motion with the positive x-axis. The time evolution of the state of any photon is then a Markov process.

Let $\Pi(M,\Lambda|x,\mu,\lambda)$ be the probability that a particle with initial state (x,μ,λ) (where $0 \le x \le a$, $-1 \le \mu \le 1$, and $0 < \lambda < \infty$) emerges from the slab with direction $\mu' \in M$ and wavelength $\lambda' \in \Lambda$. Then Π satisfies the backward Kolmogorov equation (cf. Brockwell[2] and Moyal[6]),

$$\left(\mu \frac{d}{dx} - \Sigma_\lambda\right) \Pi(x,\mu,\lambda) = - \int_{\nu=-1}^{1} \int_{\rho=0}^{2\pi} \sigma_\lambda(\theta)\Pi(x,\nu,\lambda + 1 - \cos\theta)\, d\nu d\rho \tag{2.1}$$

with boundary conditions

$$\Pi(a,\mu,\lambda) = \chi_M(\mu)\chi_\Lambda(\lambda), \quad \text{if} \quad \mu > 0, \tag{2.2}$$

$$\Pi(0,\mu,\lambda) = \chi_M(\mu)\chi_\Lambda(\lambda), \quad \text{if} \quad \mu < 0, \tag{2.3}$$

where

$$\chi_A(x) = \begin{cases} 1, & \text{if } x \in A, \\ 0, & \text{if } x \notin A, \end{cases}$$

$$\cos\theta = \mu\nu + \sqrt{(1-\mu^2)(1-\nu^2)}\cos\rho,$$

and $\sigma_\lambda(\theta)$ and Σ_λ are defined by Eqs. 1.1-1.3.

To solve Eqs. 2.1-2.3, we shall suppose (as in Brockwell[1]) that the photon is restricted to move in one of a set of 30 directions in space corresponding to the lines joining the midpoints of the edges of a regular icosahedron to its center. For a detailed account of the choice of these directions, see Ref. 2. We summarize here by observing that the directions fall into 10 classes which we denote 1, ..., 10, such that the cosine of the angle between the positive x-axis and any direction in class i is μ_i, where

$$\left.\begin{aligned} \mu_1 &= 1 &&= -\mu_{10}, \\ \mu_2 &= \tfrac{1}{4}(\sqrt{5}+1) &&= -\mu_9, \\ \mu_3 &= \tfrac{1}{2} &&= -\mu_8, \\ \mu_4 &= \tfrac{1}{4}(\sqrt{5}-1) &&= -\mu_7, \\ \mu_5 &= 0 &&= \mu_6. \end{aligned}\right\} \tag{2.4}$$

Moreover, if $\{\underset{\sim}{e}_1, \ldots, \underset{\sim}{e}_{30}\}$ denote unit vectors in the 30 possible directions of motion then for every k, the set of scalar products $\{\underset{\sim}{e}_1 \cdot \underset{\sim}{e}_k, \underset{\sim}{e}_2 \cdot \underset{\sim}{e}_k, \ldots, \underset{\sim}{e}_{30} \cdot \underset{\sim}{e}_k\}$ contains the values μ_2, μ_3, μ_4, μ_5, μ_7, μ_8, and μ_9 each repeated four times and the values μ_1 and μ_9 once only. Thus there

are precisely nine possible angular deflections, which are the same for any given initial direction. We denote these angles by $\theta_1, \ldots, \theta_9$, where

$$\left.\begin{aligned} \cos\theta_1 &= \mu_1 = -\cos\theta_9, \\ \cos\theta_2 &= \mu_2 = -\cos\theta_8, \\ \cos\theta_3 &= \mu_3 = -\cos\theta_7, \\ \cos\theta_4 &= \mu_4 = -\cos\theta_6, \\ \cos\theta_5 &= 0. \end{aligned}\right\} \tag{2.5}$$

If, conditional on the particle being scattered, we denote by p_1, $4p_2$, $4p_3$, $4p_4$, $4p_5$, $4p_6$, $4p_7$, $4p_8$, and p_9 the probabilities of deflection of the particle through $\theta_1, \theta_2, \ldots, \theta_9$, respectively, then the probabilities P_{ij} of a transition from direction i (i.e., a direction belonging to class i) to direction j (i.e., a direction belonging to class j) can be represented by the following 10×10 matrix in which P_{ij} is the jth element of the ith row:

$$P = \begin{bmatrix} (1) & (2222) & (3333) & (4444) & (55) & (55) & (6666) & (7777) & (8888) & (9) \\ (2) & (1234) & (2345) & (2356) & (46) & (37) & (4578) & (5678) & (6789) & (8) \\ (3) & (2345) & (1267) & (2457) & (28) & (46) & (3568) & (3489) & (5678) & (7) \\ (4) & (2356) & (2457) & (1368) & (37) & (28) & (2479) & (3568) & (4578) & (6) \\ (5) & (4466) & (2288) & (3377) & (19) & (55) & (3377) & (2288) & (4466) & (5) \\ (5) & (3377) & (4466) & (2288) & (55) & (19) & (2288) & (4466) & (3377) & (5) \\ (6) & (4578) & (3568) & (2479) & (37) & (28) & (1368) & (2457) & (2356) & (4) \\ (7) & (5678) & (3489) & (3568) & (28) & (46) & (2457) & (1267) & (2345) & (3) \\ (8) & (6789) & (5678) & (4578) & (46) & (37) & (2356) & (2345) & (1234) & (2) \\ (9) & (8888) & (7777) & (6666) & (55) & (55) & (4444) & (3333) & (2222) & (1) \end{bmatrix} \tag{2.6}$$

The symbol $(ijk\ell)$ is used in Eq. 2.6 as an abbreviation for the sum $p_i + p_j + p_k + p_\ell$. Clearly, the probabilities $p_1, \ldots, p_9$, and hence the matrix P, will depend on the wavelength λ of the colliding photon. When we wish to emphasize this dependence, we shall write $p_i(\lambda)$, $P(\lambda)$, etc.

Let us now consider the problem of replacing the process defined by Eqs. 1.1 and 1.2 by an approximating discrete process in which the set of possible directions of motion is restricted as just described, and moreover the wavelength of each photon is restricted to take one of a finite set of values. For a photon whose initial wavelength is λ_0, we shall restrict attention to the range of wavelengths $[\lambda_0, \lambda_{N-1}]$, dividing it into N groups, a typical one being denoted Group α, where $\alpha = 0, 1, \ldots, N - 1$. Thus,

$$\left.\begin{aligned} &\text{Group } 0 = \{\lambda_0\} \\ &\text{Group } 1 = (\lambda_0, \lambda_1] \\ &\text{Group } 2 = (\lambda_1, \lambda_2] \\ &\qquad\vdots \\ &\text{Group } N\text{-}1 = (\lambda_{N-2}, \lambda_{N-1}]. \end{aligned}\right\} \tag{2.7}$$

By truncating the range of possible wavelengths to $[\lambda_0, \lambda_{N-1}]$, we shall obtain in place of the wavelength distribution on $[\lambda_0, \infty)$ its restriction to the finite interval $[\lambda_0, \lambda_{N-1}]$. This will suffice for most purposes, provided λ_{N-1} is chosen sufficiently large.

For the discrete process, it is natural to define the collision rate $\Sigma(\alpha)$ per unit path length for a photon with wavelength α (i.e., in Group α) to be the collision rate for the original process evaluated at the midpoint of Group α; i.e.,

$$\Sigma(\alpha) = \Sigma_{\lambda^*_\alpha} = 2\pi \int_{-1}^{1} \sigma_{\lambda^*_\alpha}(\theta)\, d(\cos\theta), \tag{2.8}$$

where

$$\lambda^*_\alpha = \tfrac{1}{2}(\lambda_\alpha + \lambda_{\alpha-1}) \quad \text{if } \alpha \geq 1, \text{ and } \lambda^*_0 = \lambda_0.$$

The definition of the discrete process will then be complete once we have specified $P(\beta,j|\alpha,i)$, the probability that a scattered particle has wavelength β and direction j immediately after a collision, given that it had wavelength α and direction i immediately before the collision.

As described above, we denote by $p_1(\lambda)$, $4p_2(\lambda)$, ..., $4p_8(\lambda)$, and $p_9(\lambda)$ the probabilities, given that a particle is scattered, that it is deflected through angles θ_1, θ_2, ..., θ_8, and θ_9, respectively. Each probability $p_i(\lambda)$, $i = 1, \ldots, 9$, corresponds to the same solid angle $4\pi/30$, and so we choose the probabilities $p_i(\lambda)$ for the discrete process to satisfy

$$p_i(\lambda) = A_\lambda \sigma_\lambda(\theta_i), \tag{2.9}$$

where $\sigma_\lambda(\theta)$ is defined by Eq. 1.2, θ_i is defined by Eq. 2.5 and A_λ is chosen so that

$$p_1(\lambda) + 4\sum_{i=2}^{8} p_i(\lambda) + p_9(\lambda) = 1. \tag{2.10}$$

The required probabilities $P(\beta,j|\alpha,i)$ needed to define the discrete process are now given by

$$P(\beta,j|\alpha,i) = \sum_{k=1}^{9} P(\beta|\theta_k,\alpha)Q(j,\theta_k|\alpha,i), \tag{2.11}$$

where $P(\beta|\theta_k,\alpha)$ is the probability of a transition from wavelength group α to wavelength group β, conditional upon an angular deflection θ_k, and $Q(j,\theta_k|\alpha,i)$ is the probability, given that a particle with Group α and direction i experiences a collision, that it is deflected through an angle θ_k into direction j. The probabilities $P(\beta|\theta_k,\alpha)$ are given by

$$P(\beta|\theta_k,\alpha) = \begin{cases} \sup\left[\dfrac{\inf(\lambda_\alpha + \varepsilon_k, \lambda_\beta) - \sup(\lambda_{\alpha-1} + \varepsilon_k, \lambda_{\beta-1})}{\lambda_\alpha - \lambda_{\alpha-1}}\right], & \alpha > 0, \\ \chi_{[\lambda_{\beta-1},\lambda_\beta)}(\lambda_0 + \varepsilon_k), & \alpha = 0, \quad \varepsilon_k \neq 0, \\ \delta_{\beta,0}, & \alpha = 0, \quad \varepsilon_k = 0, \end{cases} \tag{2.12}$$

where $\delta_{\cdot,\cdot}$ is Kronecker's delta, $\chi_A(\cdot)$ is the indicator function of the set A and $\varepsilon_j = 1 - \cos\theta_j$. Equation 2.12 is derived under the assumption that the wavelength prior to the collision is *uniformly distributed* over the interval corresponding to Group α. Furthermore,

$$Q(j,\theta_k|\alpha,i) = p_k(\lambda_\alpha^*)M_{ijk}, \tag{2.13}$$

where M_{ijk} is the coefficient of p_k in P_{ij} (see Eq. 2.6). As before, λ_α^* denotes the midwavelength of Group α.

Equations 2.8 and 2.11-2.13 now determine completely a discrete analog of the original process. The analogs of Eqs. 2.1-2.3 are

$$\left[\mu_i \frac{d}{dx} - \Sigma(\alpha)\right] \Pi(x,\mu_i,\alpha) = -\Sigma(\alpha) \sum_{\beta=0}^{N-1} \sum_{j=1}^{10} \Pi(x,\mu_j,\beta)P(\beta,j|\alpha,i),$$

$$0 \leq x \leq a; \quad i = 1, \ldots, 10; \quad \alpha = 0, 1, \ldots, N-1; \tag{2.14}$$

$$\Pi(a,\mu_i,\alpha) = \chi_M(\mu_i)\chi_L(\alpha), \quad \mu_i > 0, \tag{2.15}$$

and

$$\Pi(0,\mu_i,\alpha) = \chi_M(\mu_i)\chi_L(\alpha), \quad \mu_i < 0, \tag{2.16}$$

where M is a subset of the set of direction cosines [-1,1], L is a subset of the set of groups {0, 1, ..., N - 1}, and $\Pi(x,\mu_i,\alpha)$ is the probability of emergence from the slab [0,a] with wavelength group in L and emergent direction cosine in M conditional on initial position x, direction cosine μ_i, and wavelength group α.

In the following section, we shall describe the method used to solve Eqs. 2.14-2.16.

III. THE SOLUTION OF THE BACKWARD KOLMOGOROV EQUATION FOR THE DISCRETE PROCESS

The probabilities $\Pi(M,L|x,\mu_i,\alpha)$ defined by Eqs. 2.14-2.16 can be expressed, for any sets M and L of emergent directions and wavelengths, in terms of the probabilities $\Pi(\{\mu_j\},\{\beta\}|x,\mu_i,\alpha)$ of emergence in each particular direction μ_j and wavelength group β, where $j = 1, \ldots, 4, 7, \ldots, 10$ and $\beta = 0, 1, \ldots, N-1$.

It is convenient at this point to introduce vector notation, defining a set of vectors, each with 10N components, by

$$\underline{\Pi}(\{\mu_j\},\{\beta\}|x) = \begin{bmatrix} \Pi(\{\mu_j\},\{\beta\}|x,\mu_1,0) \\ \vdots \\ \Pi(\{\mu_j\},\{\beta\}|x,\mu_1,N-1) \\ \Pi(\{\mu_j\},\{\beta\}|x,\mu_2,0) \\ \vdots \\ \Pi(\{\mu_j\},\{\beta\}|x,\mu_{10},N-1) \end{bmatrix}, \quad \begin{matrix} j = 1, \ldots, 4, 7, \ldots, 10, \\ \beta = 0, 1, \ldots, N-1. \end{matrix} \tag{3.1}$$

We also define a 10N × 8N matrix $\Gamma(x)$ whose columns are given by Eq. 3.1. Thus,

$$\Gamma(x) = [\underline{\Pi}(\{\mu_1\},\{0\}|x)\ldots\underline{\Pi}(\{\mu_1\},\{N-1\}|x)\underline{\Pi}(\{\mu_2\},\{0\}|x)\ldots\underline{\Pi}(\{\mu_{10}\},\{N-1\}|x)]. \tag{3.2}$$

The matrix $\Gamma(x)$ then contains all the relevant transition probabilities of the process, and its determination will constitute a complete solution of the scattering problem in the discrete approximation.

From Eq. 2.14, we find that the equation for $\Gamma(x)$ is

$$\left(M - D\frac{d}{dx}\right)\Gamma(x) = 0, \tag{3.3}$$

where M is a 10N × 10N matrix whose elements are directly expressible (from Eq. 2.14) in terms of $\Sigma(\alpha)$ and $P(\beta,j|\alpha,i)$, the latter being calculated as described in Sect. II. The matrix D is diagonal with elements $\mu_1, \ldots, \mu_1, \mu_2, \ldots, \mu_2, \ldots, \mu_{10}, \ldots, \mu_{10}$. In particular, the $(4N + 1)$th, $(4N + 2)$th, ..., 6Nth diagonal elements of D are zero.

In block form, we can rewrite Eq. 3.3 as

$$\begin{bmatrix} A_1 & B_1 & C_1 \\ A_2 & B_2 & C_2 \\ A_3 & B_3 & C_3 \end{bmatrix} \Gamma(x) = 0, \tag{3.4}$$

where A_1, B_2, and C_3 are square matrices of order 4N, 2N, and 4N, respectively, and A_1 and C_3 are the only submatrices in which the differential operator d/dx appears. If we denote by G(x) the 8N × 8N matrix obtained from $\Gamma(x)$ by deleting its (4N + 1)th, (4N + 2)th, ..., 6Nth rows, then it follows from Eq. 3.4 that G(x) satisfies the equation

$$\begin{bmatrix} A_1 + B_1B_2^{-1}A_2 & C_1 + B_1B_2^{-1}C_2 \\ A_3 + B_3B_2^{-1}A_2 & C_3 + B_3B_2^{-1}C_2 \end{bmatrix} G(x) = 0. \tag{3.5}$$

The matrix $\Gamma(x)$ is easily recovered from G(x) using the relation

$$[0\ B_2\ 0]\Gamma(x) + [A_2\ C_2]G(x) = 0 \tag{3.6}$$

in which the two zeros in the first factor are 2N × 4N matrices. The scattering problem will therefore be solved once we have found the 8N × 8N matrix G(x).

Equation 3.5 can be rewritten in the form

$$\frac{d}{dx} G(x) = RG(x) \tag{3.7}$$

with boundary conditions (from Eqs. 2.15 and 2.16)

$$G(0) = \begin{bmatrix} G_1 & G_2 \\ 0 & I \end{bmatrix}, \quad G(a) = \begin{bmatrix} I & 0 \\ H_1 & H_2 \end{bmatrix}, \tag{3.8}$$

where G_1, G_2, H_1, and H_2 are 4N x 4N matrices yet to be determined, and 0 and I are the 4N x 4N zero and unit matrices, respectively. The solution of Eq. 3.7 is given by

$$G(x) = e^{Rx} G(0). \tag{3.9}$$

If we partition the matrix e^{Ra} into 4N × 4N matrices T_1, T_2, T_3, and T_4, so that

$$e^{Ra} = \begin{bmatrix} T_1 & T_2 \\ T_3 & T_4 \end{bmatrix}, \tag{3.10}$$

and set x = a in Eq. 3.9, we obtain

$$\begin{bmatrix} I & 0 \\ H_1 & H_2 \end{bmatrix} = \begin{bmatrix} T_1 & T_2 \\ T_3 & T_4 \end{bmatrix} \begin{bmatrix} G_1 & G_2 \\ 0 & I \end{bmatrix}. \tag{3.11}$$

From Eq. 3.11, we find immediately that

$$G_1 = T_1^{-1}, \tag{3.12}$$

and

$$G_2 = -T_1^{-1}T_2. \tag{3.13}$$

The matrices G_1 and G_2 completely determine G(0), which in turn determines the solution G(x) via Eq. 3.9.

A FORTRAN program for the CDC-3600 computer has been written to perform the calculations described above. It is called STAM2 and is organized as a series of subroutines. The maximum-sized scattering problem that can be accommodated by the program on the two-bank CDC-3600 at present (without extensive use of external storage) is a 12-group problem, i.e., a problem with a 120 × 120 scattering matrix.

The first subroutine to be called is MANEV, which reads the scattering matrix SCAT, i.e., the 10N × 10N matrix $P(\beta,j|\alpha,i)$ of Eq. 2.14, which is generated beforehand as described in Sect. II and from it generates the 8N × 8N matrix R of Eq. 3.9.

Next, the matrix exp(aR) is calculated by subroutine EXMTR, which uses the power-series expansion of the exponential truncated according to a specified error criterion ε. If the elements of $(aR)^n/n!$, i.e., the $(n + 1)$th term of the series, are denoted by r_{ijn}, then the series is terminated after the smallest value of n for which

$$\left(\sum_{i,j} r_{ijn}^2\right)^{1/2} \leq \varepsilon..$$

The matrices G_1 and G_2 are then calculated from Eqs. 3.12 and 3.13 in subroutine PROB1. At this point, G(0) is completely determined and hence also the probabilities of emergence from the slab with any given direction and wavelength, conditional upon incidence on the left face of the slab in any one of the directions 1, ..., 4 and with any particular wavelength group. Subroutine ZDPROB determines the corresponding probabilities for the incident directions 5 and 6 parallel to the slab face. Subroutine OUTPUT1 then forms the array $\Gamma(0)$, which contains the probabilities of each possible emergent direction and wavelength conditional upon each possible incident direction and wavelength at the face x = 0. Provision is also made for calculating the probability distribution of the emergent state, conditional upon a given *distribution* of incident states. For example, if particles with wavelength λ_0 are incident isotropically on the face x = 0 of the slab, then the probability of emergence with direction j and wavelength group β is given by

$$\Pi(\{\mu_j\},\{\beta\}|0, \quad \text{Iso},0) = \sum_{i=1}^{10} r_i \Pi(\{\mu_j\},\{\beta\}|0,\mu_i,0), \tag{3.14}$$

where r_i, i = 1, ..., 10, defines the incident angular distribution corresponding to isotropic incidence, viz.,

$$r_1 = r_5 = r_6 = 1/15, \; r_2 = r_3 = r_4 = 4/15. \tag{3.15}$$

Other distributions of the incident state can be treated analogously. Marginal distributions of the emergent state are found by summing the elements of $\Gamma(0)$ over the appropriate indices. For example, the emergent angular distribution is found by summing over all emergent wavelengths; thus,

$$\Pi(\{\mu_j\}|0,\mu_i,\alpha) = \sum_{\beta=0}^{N-1} \Pi(\{\mu_j\},\{\beta\}|0,\mu_i,\alpha). \tag{3.16}$$

IV. THE LOW-ORDER-SCATTERING CORRECTION

The probabilities $\Pi(\{\mu_j\},\{\beta\}|x,\mu_i,\alpha)$ of emergence with direction j and wavelength group β conditional on initial position x, direction i, and wavelength group α can be decomposed according to the number of collisions experienced by the particle before emergence. Thus,

$$\Pi(\{\mu_j\},\{\beta\}|x,\mu_i,\alpha) = \sum_{n=0}^{\infty} \Pi_n(\{\mu_j\},\{\beta\}|x,\mu_i,\alpha).$$

Since we are using the discrete process only as an approximation to the continuous state-space process described in Sect. I, and since it is possible for the continuous process to calculate directly the zero-scattering and single-scattering components of the distribution of emergent direction and wavelength, we use the discrete approximation only to calculate

$$\sum_{n=2}^{\infty} \Pi_n(\{\mu_j\},\{\beta\}|x,\mu_i,\alpha).$$

Subroutine COREC evaluates the probabilities $\Pi_0(\{\mu_j\},\{\beta\}|0,\mu_i,\alpha)$ and $\Pi_1(\{\mu_j\},\{\beta\}|0,\mu_i,\alpha)$ for the discrete process and subtracts them from $\Pi(\{\mu_j\},\{\beta\}|0,\mu_i\alpha)$ to obtain the probabilities of emergence with at least two scattering collisions, denoted by $\Pi_{2+}(\{\mu_j\},\{\beta\}|0,\mu_i,\alpha)$. The marginal distributions of Π_{2+} and the corresponding probabilities conditional on some *distribution* of incident states are calculated precisely as described at the end of Sect. III.

Finally the distribution Π_{2+}, derived on the basis of the discrete approximation, is combined with the zero- and single-scattering components as calculated directly for the continuous process. Separate computer programs have been developed to perform these direct calculations, and they will now be described.

We introduce the conditional probability density $q_1(\nu,\Delta|\mu,\lambda)$ defined by

$q_1(\nu,\Delta|\mu,\lambda)\, d\nu d\Delta$ = Probability {a particle with incident direction cosine μ and wavelength λ emerges with direction cosine in the interval $(\nu, \nu + d\nu)$ and wavelength in the interval $(\lambda + \Delta, \lambda + \Delta + d\Delta)$ after experiencing exactly one collision in the slab}.

Note that q_1 does not exist as a density in the particular case $\mu = 1$. We shall restrict attention here to *transmitted* radiation, so that $\nu > 0$ and $\mu > 0$. (Reflected radiation can be dealt with quite analogously.) The density q_1 is then given, for $\mu \neq 1$, by

$$q_1(\nu,\Delta|\mu,\lambda) = \begin{cases} \dfrac{2\nu\sigma(\Delta,\lambda)[\mu\Sigma_{\lambda+\Delta} - \nu\Sigma_\lambda]^{-1}}{[(1-\mu^2)(1-\nu^2) - (\Delta - 1 + \mu\nu)^2]^{1/2}} \{\exp(-\Sigma_\lambda t/\mu) - \exp(-\Sigma_{\lambda+\Delta} t/\nu)\}, \\ \qquad\qquad \text{if } \mu\Sigma_{\lambda+\Delta} \neq \nu\Sigma_\lambda, \\ t\exp(-\Sigma_\lambda t/\mu), \quad \text{if } \mu\Sigma_{\lambda+\Delta} = \nu\Sigma_\lambda, \end{cases} \tag{4.1}$$

provided $(1 - \mu^2)(1 - \nu^2) - (\Delta - 1 + \mu\nu)^2 > 0$. If this condition is not satisfied, then $q_1(\nu,\Delta|\mu,\lambda) = 0$. In Eq. 4.1, t denotes the thickness of the slab measured in units of the limiting mean free path at zero energy (or infinite wavelength), while

$$\sigma(\Delta,\lambda) = \frac{3}{16\pi}\left[\frac{\lambda}{\lambda+\Delta} + \frac{\lambda+\Delta}{\lambda} - 1 + (\Delta - 1)^2\right]\left[\frac{\lambda}{\lambda+\Delta}\right]^2 \tag{4.2}$$

and

$$\Sigma_\lambda = \frac{3}{4}\left\{(\lambda^2 + \lambda)\left[\frac{2(\lambda+1)}{\lambda+2} - \log\frac{\lambda+2}{\lambda}\right] + \frac{\lambda}{2}\log\frac{\lambda+2}{2} - \frac{\lambda^2+3}{(\lambda+2)^2}\right\}. \tag{4.3}$$

The computer program SINGLE2 evaluates the probability density in Eq. 4.1 for specified λ and μ and from it computes the singly scattered transmitted spectral density given by

$$F_1(\Delta|\mu,\lambda) = \int_A^B q_1(\nu,\Delta|\mu,\lambda)\, d\nu, \tag{4.4}$$

where

$$A = \max\{0,\ \mu(1-\Delta) - [\Delta(2-\Delta)(1-\mu^2)]^{1/2}\}$$

and

$$B = \max\{0,\ \min(1,\ \mu(1-\Delta) + [\Delta(2-\Delta)(1-\mu^2)]^{1/2})\}.$$

The integral in Eq. 4.4 is singular; however, it can be reduced to a nonsingular integral by breaking the range of integration into two parts and making changes of variable in each. For the particular incident direction $\mu = 1$, the density $F_1(\Delta|1,\lambda)$ must be calculated directly from the equation

$$F_1(\Delta|1,\lambda) = \begin{cases} \dfrac{2\pi\sigma(\Delta,\lambda)(1-\Delta)}{\Sigma_{\lambda+\Delta} - \Sigma_\lambda(1-\Delta)} \{\exp(-\Sigma_\lambda t) - \exp(-\Sigma_{\lambda+\Delta} t/[1-\Delta])\} \\ \qquad\qquad \text{if } \Sigma_{\lambda+\Delta} \neq (1-\Delta)\,\Sigma_\lambda, \\ t\exp(-\Sigma_\lambda t) \quad \text{if } \Sigma_{\lambda+\Delta} = (1-\Delta)\,\Sigma_\lambda. \end{cases} \tag{4.5}$$

The program also calculates the spectral density for a *distribution* of incident directions. In particular, we have calculated

$$F_1(\Delta|g,\lambda) = \int_0^1 g(\mu) F_1(\Delta|\mu,\lambda)\, d\mu \tag{4.6}$$

for $g(\mu) = 1$, $0 \leq \mu \leq 1$ (isotropic incidence) and for $g(\mu) = 2\mu$, $0 \leq \mu \leq 1$ (cosine incidence).

The marginal distribution of emergent direction for singly scattered photons is calculated by program SINGLE3. The marginal probability density is given by

$$h_1(\nu|\mu,\lambda) = \int_a^b q_1(\nu,\Delta|\mu,\lambda)\, d\Delta \tag{4.7}$$

with

$$a = 1 - \mu\nu - [(1-\mu^2)(1-\nu^2)]^{1/2}$$

and

$$b = 1 - \mu\nu + [(1-\mu^2)(1-\nu^2)]^{1/2}.$$

The density $h_1(\nu|\mu,\lambda)$ is calculated for specified values of the incident direction and wavelength, μ and λ, and also for various distributions of incident direction. In particular, we have calculated

$$h_1(\nu|g,\lambda) = \int_0^1 g(\mu) h_1(\nu|\mu,\lambda)\, d\mu \tag{4.8}$$

for $g(\mu) = 1$ and $g(\mu) = 2\mu$, $\quad 0 \leq \mu \leq 1$.

As in Eq. 4.4, the integral defining h_1 is singular. However, by breaking the range of integration into two parts and making a change of variable, we can transform it into a nonsingular integral suitable for numerical integration.

For the particular case $\mu = 1$, $h_1(\nu|1,\lambda)$ is calculated by using the relation

$$h_1(\nu|1,\lambda) = F_1(1 - \nu|1,\lambda), \tag{4.9}$$

where $F_1(1 - \nu|1,\lambda)$ is given by Eq. 4.5.

Notice that we have not discussed the calculation of the transmitted probability densities for unscattered particles. It is a trivial matter to express these in terms of Dirac delta functions. Consequently, we restrict attention to particles that are scattered at least once (diffuse" radiation in the terminology of Chandrasekhar[3]).

There remains the problem of interpreting the n-collision probabilities $\Pi_n(\{\mu_j\},\{\beta\}|x,\mu_i,\alpha)$, $n \geq 2$, for the *discrete* process (see Eq. 4.1) in terms of the corresponding probability densities $q_n(\mu,\lambda|x,\mu_0,\lambda_0)$ for the *continuous* process in order to combine them with the single-scattered probability density $q_1(\mu,\lambda|x,\mu_0,\lambda_0)$. To achieve this, we use the following estimates for q_n, $n \geq 2$:

$$\hat{q}_n(\mu_j,\lambda^*_\beta|x,\mu_i,\lambda^*_\alpha) = \frac{K_j}{\lambda_\beta - \lambda_{\beta-1}} \Pi_n(\{\mu_j\},\{\beta\}|x,\mu_i,\alpha), \quad \beta = 1, \ldots, N-1, \tag{4.10}$$

where

$$K_j = \begin{cases} 3.75, & j = 2,3,4,7,8,9, \\ 15, & j = 1,10, \\ 0, & j = 5,6, \end{cases} \tag{4.11}$$

and λ_β and λ^*_β are defined in Eqs. 2.7 and 2.8. Equation 4.10 is derived by assuming that the emergent direction has a density that is piecewise constant on the unit sphere for each wavelength, and that the emergent wavelength has a piecewise constant density for each direction. The significance of the constants K_j is explained in Ref. 2.

The marginal densities are estimated similarly. Thus the density with respect to wavelength of the probability of transmission after exactly n collisions is estimated by

$$\hat{F}_n(\lambda^*_\beta|0,\mu_i,\lambda^*_\alpha) = \frac{1}{\lambda_\beta - \lambda_{\beta-1}} \sum_{j=1}^{4} \Pi(\{\mu_j\},\{\beta\}|0,\mu_i,\alpha), \tag{4.12}$$

and the corresponding density with respect to emergent direction-cosine by

$$\hat{h}_n(\mu_j|0,\mu_i,\lambda^*_\alpha) = K_j \sum_{\beta=1}^{N-1} \Pi(\{\mu_j\},\{\beta\}|0,\mu_i,\alpha). \tag{4.13}$$

Equations 4.10, 4.12, and 4.13 can now be used in conjunction with Eqs. 4.1, 4.4, and 4.7 to give the probability density of the emergent state of transmitted photons which are scattered at least once, viz.,

$$q_{1+}(\mu_j,\lambda_\beta^*|0,\mu_i,\lambda_\alpha^*) = q_1(\mu_j,\lambda_\beta^*|0,\mu_i,\lambda_\alpha^*) + \sum_{n=2}^{\infty} \hat{q}_n(\mu_j,\lambda_\beta^*|0,\mu_i,\lambda_\alpha^*), \quad (4.14)$$

$$F_{1+}(\lambda_\beta^*|0,\mu_i,\lambda_\alpha^*) = F_1(\lambda_\beta^*|0,\mu_i,\lambda_\alpha^*) + \sum_{n=2}^{\infty} \hat{F}_n(\lambda_\beta^*|0,\mu_i,\lambda_\alpha^*), \quad (4.15)$$

$$h_{1+}(\mu_j|0,\mu_i,\lambda_\alpha^*) = h_1(\mu_j|0,\mu_i,\lambda_\alpha^*) + \sum_{n=2}^{\infty} \hat{h}_n(\mu_j|0,\mu_i,\lambda_\alpha^*), \quad (4.16)$$

where q_1, F_1, and h_1 are based on direct calculation and

$$\sum_{n=2}^{\infty} \hat{q}_n, \quad \sum_{n=2}^{\infty} \hat{F}_n \text{ and } \sum_{n=2}^{\infty} \hat{h}_n$$

are based on the discrete approximation.

V. NUMERICAL RESULTS

A. Single-scattering Calculations

Figure 1 shows the probability density $h_1(\mu|\text{Iso},\lambda)$, $0 \le \mu \le 1$, of the emergent direction cosine of singly-scattered transmitted photons for a slab of thickness 2/3 and for photons that are incident istropically on the slab with initial wavelengths λ = 0.25, 1.0, and 50.0.

Figure 2 shows the probability density $F_1(\Delta|\text{Iso},\lambda)$ of the *increase* in wavelength of singly-scattered transmitted photons for the same slab thickness, 2/3, isotropic incidence, and initial wavelengths λ = 0.25, 1.0, and 50.0.

To illustrate the magnitude of the correction involved in replacing the discrete approximation to the singly-scattered component by its exact value, we show in Figs. 3 and 4 the single-scattered marginal densities of direction cosine and wavelength together with the corresponding discrete approximations. (The circled points are the discrete approximations.)

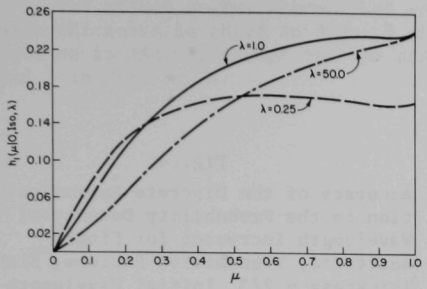

Fig. 1

The Probability Density of the Emergent Direction Cosine of Singly-scattered, Transmitted Photons; Slab Thickness = 2/3, Initial Wavelength = λ, Isotropic Incidence. The area under each curve is the probability of transmission with exactly one scattering collision.

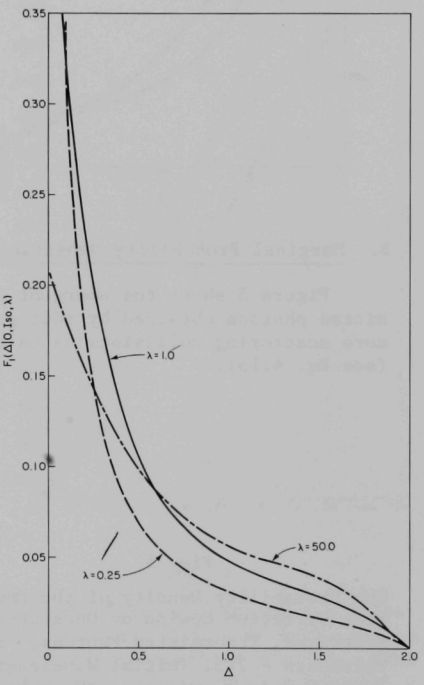

Fig. 2

The Probability Density of the Wavelength Increment of Singly-scattered, Transmitted Photons; Slab Thickness = 2/3, Initial Wavelength = λ, Isotropic Incidence. The area under each curve is the probability of transmission with exactly one scattering collision.

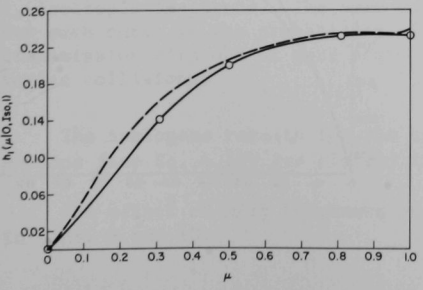

Fig. 3

Accuracy of the Discrete Approximation to the Probability Density of Emergence Direction Cosine for Singly-scattered, Transmitted Photons; Slab Thickness = 2/3, Initial Wavelength = 1, Isotropic Incidence. The circled points are those obtained from the discrete approximation; the broken curve represents the exact values.

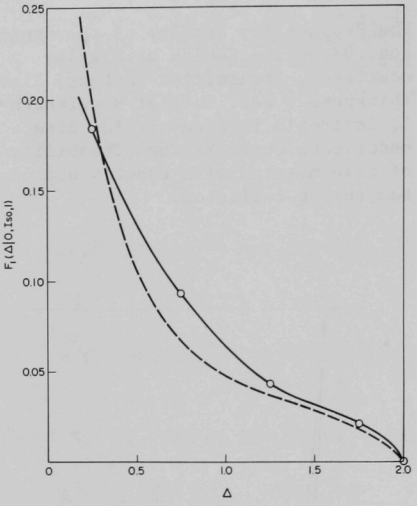

Fig. 4

Accuracy of the Discrete Approximation to the Probability Density of Wavelength Increment for Singly-scattered, Transmitted Photons; Slab Thickness = 2/3, Initial Wavelength = 1, Isotropic Incidence. The circled points are those obtained from the discrete approximation; the broken curve represents the exact values.

B. Marginal Probability Densities for Diffusely Transmitted Photons

Figure 5 shows the emergent angular distribution of diffusely transmitted photons obtained by adding to Fig. 1 the contributions from two and more scattering collisions as calculated from the discrete approximation (see Eq. 4.15).

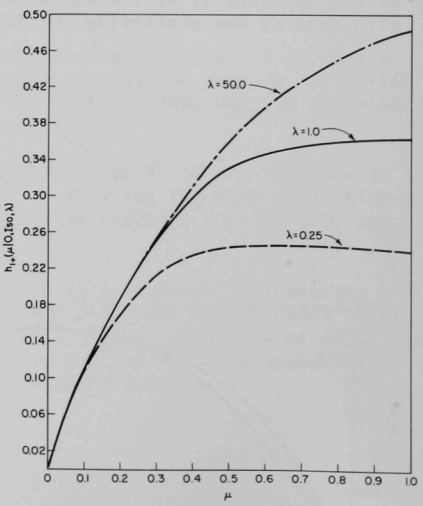

Fig. 5

The Probability Density of the Emergent Direction Cosine of Once-or-more Scattered, Transmitted Photons; Slab Thickness = 2/3, Initial Wavelength = λ, Isotropic Incidence. The area under each curve is the probability of transmission with one or more scattering collisions.

The effect on the transmitted angular distribution of varying the slab thickness is shown in Figs. 6 and 7. The parameters are all kept the same as in Fig. 5, except for the slab thickness, which is 4/3 in Fig. 6 and 2 in Fig. 7.

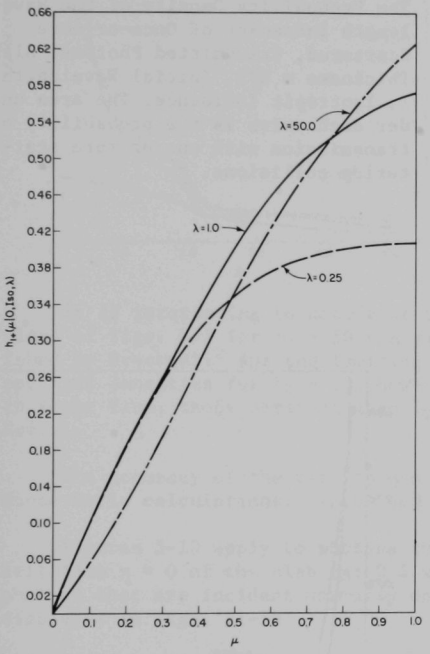

Fig. 6

The Probability Density of the Emergent Direction Cosine of Once-or-more Scattered, Transmitted Photons; Slab Thickness = 4/3, Initial Wavelength = λ, Isotropic Incidence. The area under each curve is the probability of transmission with one or more scattering collisions.

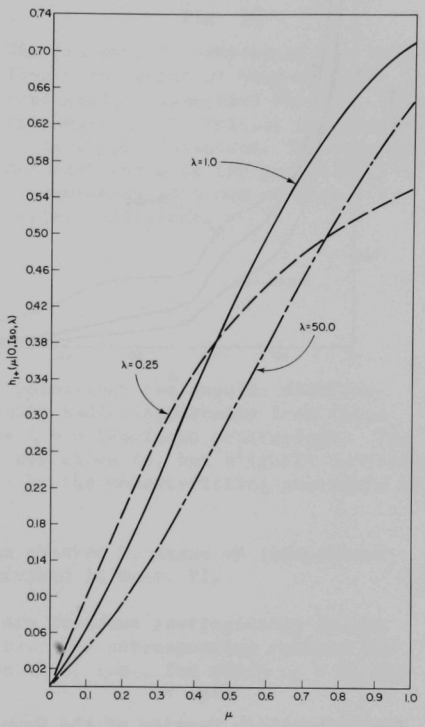

Fig. 7

The Probability Density of the Emergent Direction Cosine of Once-or-more Scattered, Transmitted Photons; Slab Thickness = 2.0, Initial Wavelength = λ, Isotropic Incidence. The area under each curve is the probability of transmission with one or more scattering collisions.

The analogous results for the spectral density of diffusely transmitted photons (see Eq. 4.16) are plotted in Fig. 8.

The effect of slab thickness on the transmitted spectral density is shown in Figs. 9 and 10.

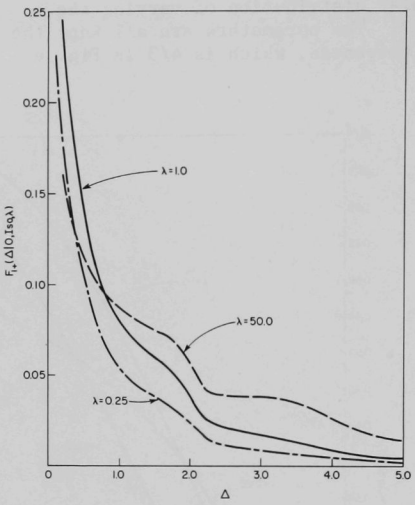

Fig. 8

The Probability Density of the Wavelength Increment of Once-or-more Scattered, Transmitted Photons; Slab Thickness = 2/3, Initial Wavelength = λ, Isotropic Incidence. The area under each curve is the probability of transmission with one or more scattering collisions.

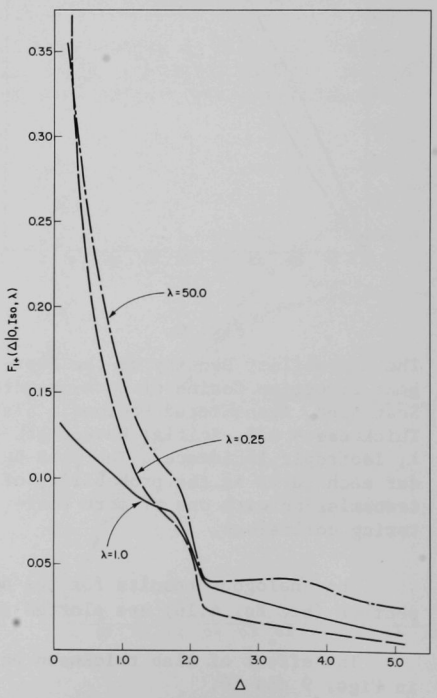

Fig. 9

The Probability Density of the Wavelength Increment of Once-or-more Scattered, Transmitted Photons; Slab Thickness = 4/3, Initial Wavelength = λ, Isotropic Incidence. The area under each curve is the probability of transmission with one or more scattering collisions.

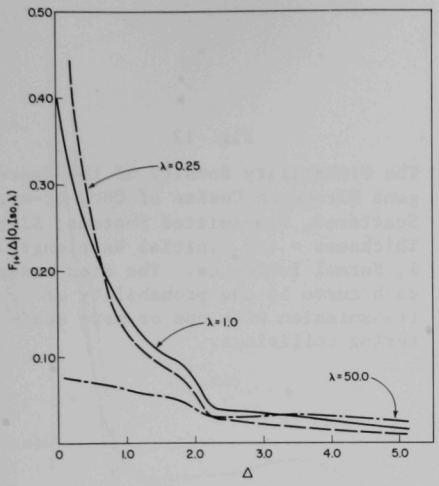

Fig. 10

The Probability Density of the Wavelength Increment of Once-or-more Scattered, Transmitted Photons; Slab Thickness = 2.0, Initial Wavelength = λ, Isotropic Incidence. The area under each curve is the probability of transmission with one or more scattering collisions.

It is interesting to notice at this point that the angular distributions of Figs. 5-7 for $\lambda_0 = 50$ are virtually indistinguishable from those found by Brockwell[2] for the limiting case $\lambda = \infty$ (Rayleigh scattering). The spectral densities for $\lambda_0 = 50$, however, are close to, but slightly different in shape from, those obtained when $\lambda_0 = \infty$ by the moment-fitting procedure of Ref. 1.

The accuracy of the results has been checked by means of independent Monte Carlo calculations. These are described in Sect. VI.

Figures 5-10 apply to photons that are incident isotropically on the left face x = 0 of the slab $\{x: 0 \leq x \leq t\}$. The corresponding results for photons that are incident *normally* on the slab, i.e., for which $\mu_0 = 1$, are displayed in Figs. 11-16.

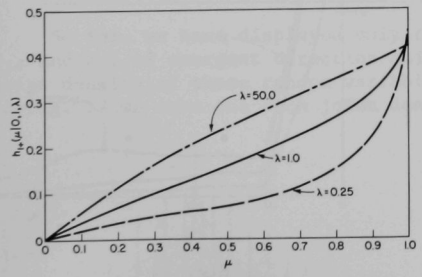

Fig. 11

The Probability Density of the Emergent Direction Cosine of Once-or-more Scattered, Transmitted Photons; Slab Thickness = 2/3, Initial Wavelength = λ, Normal Incidence. The area under each curve is the probability of transmission with one or more scattering collisions.

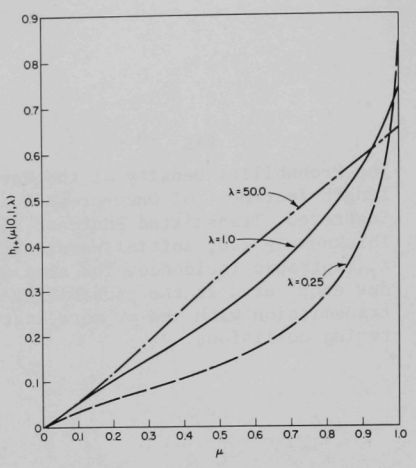

Fig. 12

The Probability Density of the Emergent Direction Cosine of Once-or-more Scattered, Transmitted Photons; Slab Thickness = 4/3, Initial Wavelength = λ, Normal Incidence. The area under each curve is the probability of transmission with one or more scattering collisions.

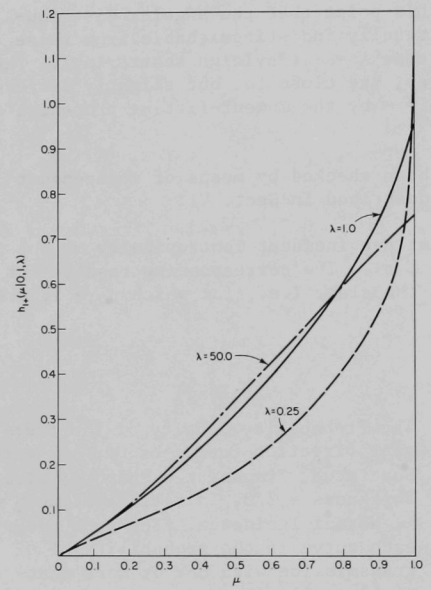

Fig. 13

The Probability Density of the Emergent Direction Cosine of Once-or-more Scattered, Transmitted Photons; Slab Thickness = 2.0, Initial Wavelength = λ, Normal Incidence. The area under each curve is the probability of transmission with one or more scattering collisions.

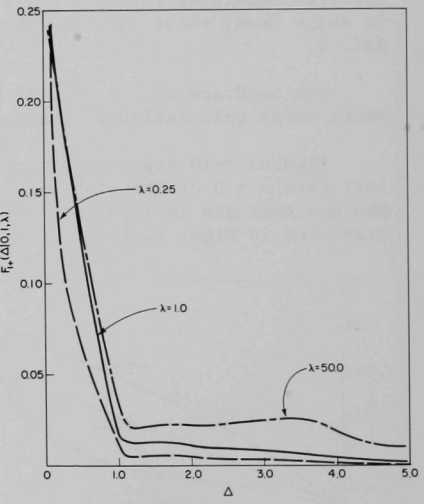

Fig. 14

The Probability Density of the Wavelength Increment of Once-or-more Scattered, Transmitted Photons; Slab Thickness = 2/3, Initial Wavelength = λ, Normal Incidence. The area under each curve is the probability of transmission with one or more scattering collisions.

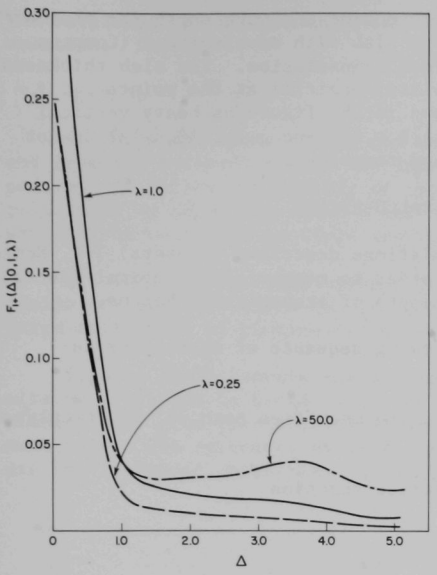

Fig. 15

The Probability Density of the Wavelength Increment of Once-or-more Scattered, Transmitted Photons; Slab Thickness = 4/3, Initial Wavelength = λ, Normal Incidence. The area under each curve is the probability of transmission with one or more scattering collisions.

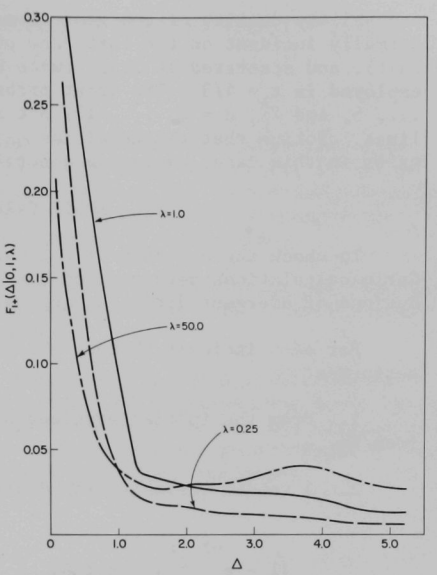

Fig. 16

The Probability Density of the Wavelength Increment of Once-or-more Scattered, Transmitted Photons; Slab Thickness = 2.0, Initial Wavelength = λ, Normal Incidence. The area under each curve is the probability of transmission with one or more scattering collisions.

C. The Joint Probability Density of Emergent Direction and Wavelength

So far, we have displayed only the *marginal* probability densities h_{1+} and F_{1+} of emergent direction and wavelength, respectively. However, the joint density of these random variables is also available through Eq. 4.14. In Fig. 17 we show one such joint density, $q_{2+}(\mu_j,\lambda_\beta^*|0,1,1)$, i.e., the

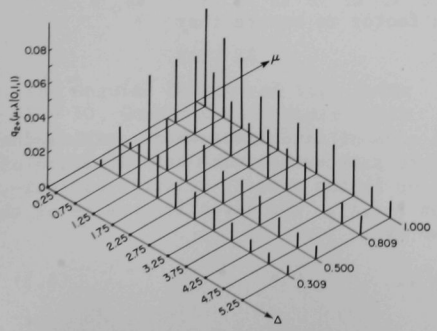

Fig. 17

The Joint Density of Emergent Direction Cosine and Wavelength Increment for Twice-or-more Scattered, Transmitted Photons; Slab Thickness = 4/3, Initial Wavelength = 1.0, Normal Incidence.

probability density of emergent direction cosine and wavelength for photons normally incident on the left face of the slab with wavelength 1 (Compton unit), and scattered at least twice before transmission. The slab thickness employed is $t = 4/3$. The joint probability densities at the points μ_j, $j = 1, \ldots, 5$, and λ^*_β, $\beta = 1, \ldots, 12$, are shown in the figure as heavy vertical lines. Notice that the densities $q_0(\nu,\lambda|0,\mu,\lambda_0)$ and $q_1(\nu,\lambda|0,\nu,\lambda_0)$ do not exist in this case, except as generalized functions.

VI. MONTE CARLO CALCULATIONS

To check the accuracy of the calculations described in Sects. I-V, Monte Carlo calculations were carried out in order to measure the marginal distributions of emergent direction and wavelength of transmitted photons.

For each incident photon, the following sequence of operations is performed:

1. From the initial wavelength λ_0, the mean free path $\Sigma^{-1}_{\lambda_0}$ is calculated from Eq. 4.3.

2. A random variable with distribution function

$$F(x) = \begin{cases} 1 - e^{-\Sigma_{\lambda_0} x}, & x \geq 0, \\ 0, & x < 0, \end{cases} \tag{6.1}$$

is generated. This represents the distance traveled by the photon before its first collision. The projection on the normal to the slab face of this distance is calculated from the initial direction of motion of the photon (which has direction cosine μ_0, say).

3. If the particle leaves the slab without first making a collision, then it is counted as an unscattered photon and a new incident photon is sampled. If the particle makes a collision at some point inside the slab, then the cosine of the angular deflection is sampled using the probability density

$$f(c) = K \frac{\lambda_0^2}{(\lambda_0+1-c)^2} \left[\frac{\lambda_0}{\lambda_0+1-c} + \frac{\lambda_0+1-c}{\lambda_0} + 1 - c^2 \right], \quad -1 \leq c \leq 1. \tag{6.2}$$

(The constant K is just a normalization factor to ensure that

$$\int_{-1}^{1} f(c)dc = 1.)$$

The angular deflection $\cos^{-1}c$ defines a cone of directions whose axis is the direction of motion of the particle before scattering. The new direction of motion is chosen from among the directions in the cone by selecting an azimuthal angle ϕ, uniformly distributed on $[-\pi,\pi]$. The direction cosine of the new direction of motion μ_1 is then given by

$$\mu_1 = \mu_0 c - \sqrt{(1 - \mu_0^2)(1 - c^2)} \cos \phi. \tag{6.3}$$

The wavelength of the photon after scattering is obtained from the Compton relation. Thus,

$$\lambda_1 = \lambda_0 + 1 - c. \tag{6.4}$$

4. From the direction μ_1 and wavelength λ_1 after the first collision and from the x-coordinate of the location of the first collision, it is now possible to follow the history of the photon through the second and subsequent collisions by repeating steps 2 and 3 with the appropriate directions and wavelengths until the particle eventually emerges from the slab.

5. When the particle emerges from the slab, its wavelength and direction cosine are recorded and a new incident particle sampled until a sufficiently large collection of photons has been observed.

Figures 18-25 compare the marginal densities F_{1+} and h_{1+} obtained as already described in Sects. I-V, and the results of corresponding Monte Carlo simulations. The points obtained from the Monte Carlo method are circled in each case. The agreement between the two methods is very good. Figures 18-21 are for isotropic incidence, and Figs. 22-25 for normal incidence.

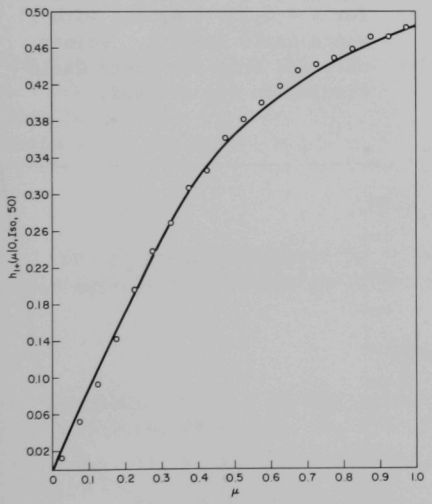

Fig. 18

The Angular Density of Fig. 5 for $\lambda = 50$, Compared with Monte Carlo Results. Points obtained from the Monte Carlo simulation are circled.

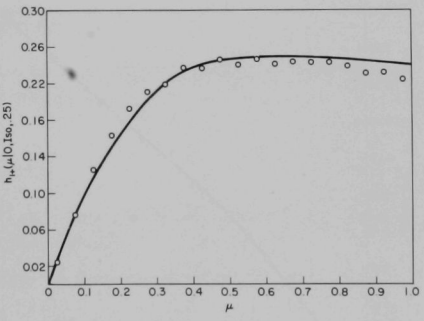

Fig. 19

The Angular Density of Fig. 5 for $\lambda = 0.25$, Compared with Monte Carlo Results. Points obtained from the Monte Carlo simulation are circled.

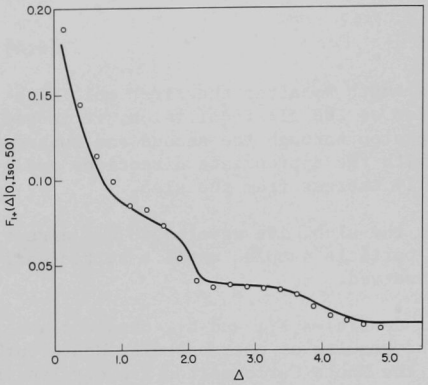

Fig. 20

The Spectral Density of Fig. 8 for $\lambda = 50$, Compared with Monte Carlo Results. Points obtained from the Monte Carlo simulation are circled.

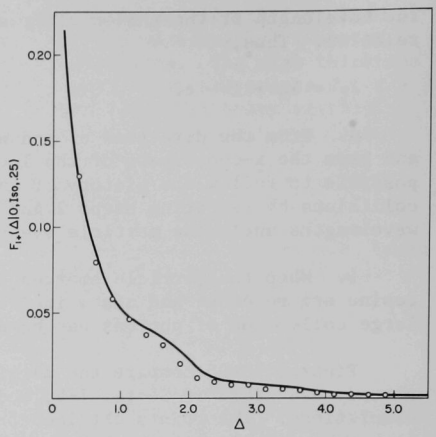

Fig. 21

The Spectral Density of Fig. 8 for $\lambda = 0.25$, Compared with Monte Carlo Results. Points obtained from the Monte Carlo simulation are circled.

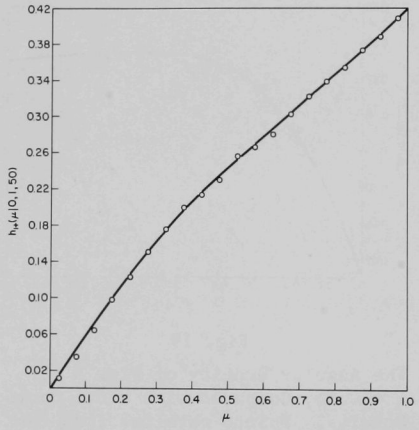

Fig. 22

The Angular Density of Fig. 11 for $\lambda = 50$, Compared with Monte Carlo Results. Points obtained from the Monte Carlo simulation are circled.

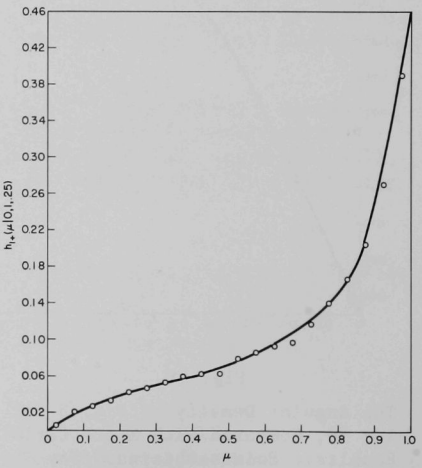

Fig. 23

The Angular Density of Fig. 11 for $\lambda = 0.25$, Compared with Monte Carlo Results. Points obtained from the Monte Carlo simulation are circled.

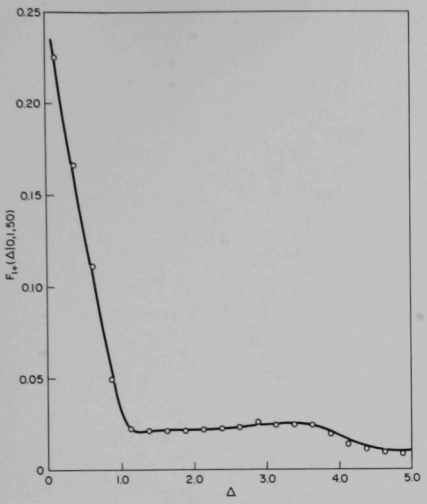

Fig. 24

The Spectral Density of Fig. 14 for $\lambda = 50$, Compared with Monte Carlo Results. Points obtained from the Monte Carlo simulation are circled.

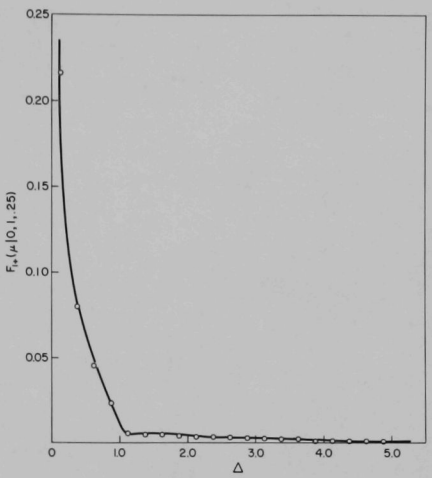

Fig. 25

The Spectral Density of Fig. 14 for $\lambda = 0.25$, Compared with Monte Carlo Results. Points obtained from the Monte Carlo simulation are circled.

ACKNOWLEDGMENT

We are greatly indebted to J. E. Moyal for many valuable discussions and suggestions in connection with this work.

REFERENCES

1. Brockwell, P. J., *The Multiple Compton Scattering of Low-energy Gamma-radiation*, Phil. Mag. *12*, 117, 508-518 (1965).

2. Brockwell, P. J., *Stochastic Problems in Transport Theory*, ANL-7131 (1966).

3. Chandrasekhar, S., *Radiative Transfer*, 2nd ed., Dover Publications, Inc., New York (1960).

4. Chandrasekhar, S., *The Softening of Radiation by Multiple Compton Scattering*, Proc. Roy. Soc. (London) *A192*, 508 (1946).

5. Fano, U., Spencer, L. V., and Berger, M. J., *Penetration and Diffusion of X-rays*, Handbuch der Physik *38*(2), Springer Verlag, Berlin (1959).

6. Moyal, J. E., *A General Theory of First-passage Processes and Transport and Multiplicative Processes*, J. Math. Phys. *7*, 464-473 (1966).

7. O'Rourke, R. C., *Multiple Compton-scattering of Low-energy Gamma-radiation*, Phys. Rev. *85*, 881-885 (1952).